ACS OMEGA

http://pubs.acs.org/journal/acsodf

Article

Study of Combustion Characteristics and Kinetics of Agriculture Briquette Using Thermogravimetric Analysis

Jianbiao Liu, Xuya Jiang, Hongzhen Cai,* and Feng Gao

Cite This: *ACS Omega* 2021, 6, 15827−15833

Read Online

ACCESS | Metrics & More | Article Recommendations

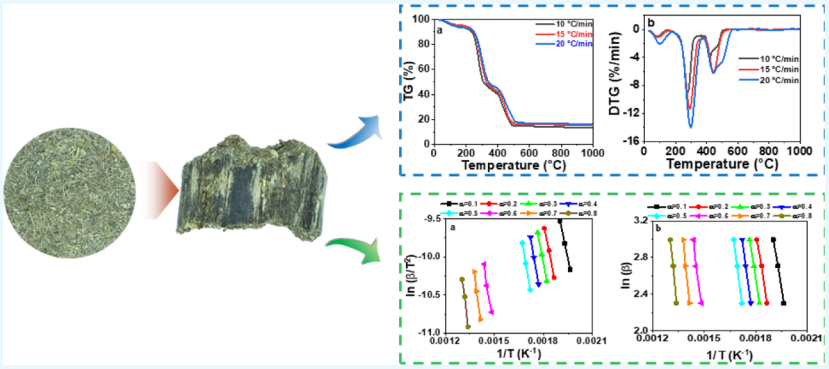

ABSTRACT: The present paper was aimed to investigate the physicochemical properties and combustion characteristics of corn straw briquette as a fuel energy. The results of physicochemical properties displayed that corn straw briquette has higher volatile matter, lower ash content, and higher heating value. Combustion characteristics and kinetic analysis were investigated using thermogravimetry analysis at various heating rates of 10, 15, and 20 °C/min. It was observed that the maximum burning rate shifted to a higher temperature as the heating rate increased. In addition, a lower heating rate would help in better heat transfer, leading to less mass residual. In contrast, the combustion characteristic index showed a nearly 2-fold increase under a higher heating rate, indicating a good combustion performance. The combustion kinetics were expressed using isoconversional methods with Kissinger−Akahira−Sunose and Ozawa−Flynn−Wall methods, which authenticated the average activation energy at 108.85 and 114.42 kJ/mol, respectively. These results can provide a theoretical basis and data support for further utilization of agriculture biomass briquette.

1. INTRODUCTION

Facing a serious challenge of the shortage problem of fossil energy coupled with environmental degradation has made the awareness of the development of alternative energy sources an urgent matter. Among various forms of renewable energy, biomass has captured attention for its huge resources, low cost, renewable nature, and low emissions.[1−3] It can also become the future source of energy for its low carbon dioxides and sulfur oxides than fossil fuels.[4] Biomass ranks fourth after coal, oil, and gas, providing approximately 14% of the global energy demand.[5] Agriculture and forestry residues, livestock manure, municipal solid waste, sewage, wastewater, and energy plants are the main sources of biomass. China is an agricultural country, and a large amount of biomass is produced every year, which equals 460 million tons of standard coal.[1] However, the low density and high costs of handling, transportation, and storage restricted its further utilization.[6−9] They are combusted directly without the optimization of energy efficiency, or they are left on farming area, potentially causing loss of energy and air and water pollution.[10] One effective way to solve these problems is densification of biomass into pellet or briquette. More generally, it is a physical change process of the crushed irregular shape biomass material rearranged by the mechanical and plastic deformation under specific temperature, pressure, and moisture content. Compared to raw material, the made pellet or briquette has the advantage of higher density and heating value, lower carbon dioxide and sulfur dioxide emissions, and reducing release of toxic and greenhouse gases. Meanwhile, the increased density and decreased volume reduce transport and storage costs.

Nowadays, some rural areas in China are using scattered coal for heating. However, the emissions were 10 times that of coal-fired power plants. One or more China policies point to focus on the development of biomass heating, while solving the

Received: March 8, 2021
Accepted: May 25, 2021
Published: June 9, 2021

Table 1. Ultimate and Proximate Analysis

	ultimate analysis (%)					proximate analysis (%)			
item	C	H	O	N	S	moisture	volatile matter	fixed carbon	ash
CSB	42.95	6.68	40.82	0.71	0	10.20	69.65	11.31	8.84

environmental problems caused by the direct burning of scattered coal and agroforestry waste. Hence, the utilization of pellets or briquette fuel as an alternative fuel has a well future. However, accurate combustion kinetic models are essential to the full utilization. Combustion kinetics focuses on the combustion reaction mechanism, combustion reaction rate, and influencing factors, which will help to predict the combustion efficiency, combustion parameters, and pollutant emissions. It can provide an accurate chemical mechanism for the actual combustion situation and optimize the burner structure and operation parameters.

Thermogravimetry analysis (TGA) is one of the most common methods and has received great attention in the understanding of solid fuel substrate degradation to release energy.[11] In addition, some studies have been carried out on the combustion characteristics of biomass solid fuel and biomass blends, such as cotton refuse,[12] pine and corn straw,[13] microalgal,[14] pinewood sawdust,[15] Azadirachta indica seeds and Phyllanthus emblica kernel,[16] red pepper,[17] rice husk,[18] camphor,[19] elephant grass,[20] hazelnut husk,[4] soybean straw,[21] and banana peel.[22]

As mentioned above, researchers mostly focus on the study of biomass materials or pellets, while rarely mentioning the biomass briquette. Subsequently, the present paper purposed to enrich the studies to analyze the combustion characteristics of biomass fuel. In this paper, TGA was applied to evaluate the combustion characteristics of corn straw briquette at a heating rate of 10, 15, 20 °C/min. The isoconversional methods, Kissinger−Akahira−Sunose (KAS) and Ozawa−Flynn−Wall (OFW), were used for calculating kinetic parameters. The results can be provided for further utilization and thermochemical conversion of agriculture biomass briquettes.

2. RESULTS AND DISCUSSION

2.1. Biomass Briquette Characteristics. Various studies confirmed that the thermochemical process largely depends on biomass characteristics.[23−26] High volatile content matter facilitates the formation of more pyrolytic liquid and gaseous products. McKendry reported that the lower the ratios of O/C and H/C are, the greater the energy content of the biomass is.[24] In addition, studies showed that less amount of N and S made it more environmentally friendly. Table 1 presents the proximate and ultimate analysis of the CSB. As can be seen from Table 1, the moisture content was 10.20%, indicating their suitability for combustion because the moisture content was around 10%.[27] The amount of volatile matter in the CSB has 69.65%. The volatile matter can affect the ignition temperature during combustion.[28] Thus, the CSB can ignite earlier and burn faster. It can also be observed that CSB has lower ash content, 8.84%. An unfavorable relationship between higher ash content and combustion tends to make poor combustion, lower heating value, as well as slagging, which is harmful to the furnace.

In addition, the ultimate analysis results showed that the main components were C and O elements, which were shown to be 42.95 and 40.82%. Higher O content was mainly because of the highly oxygenated content, such as cellulose, hemicellulose, lignin, and other substances.[23] The H/C and O/C ratio is 0.15 and 0.95, respectively, resulting in an HHV of 16.79 MJ/kg, which is higher than the heating value of the pellet obtained in our previous literature.[29] Thus, the made briquette can be considered to be a good fuel energy resource. However, the H, N, and S elements were found to be lower, total less than 10%. The lower N and trace S content reflected the low *NOx* and *SOx* emissions during combustion. It also indicated that the CSB is a valuable fuel for thermal utilization.

2.2. Thermogravimetric Analysis. TGA has been a mature technique for studying combustion behavior.[30] Figure 1

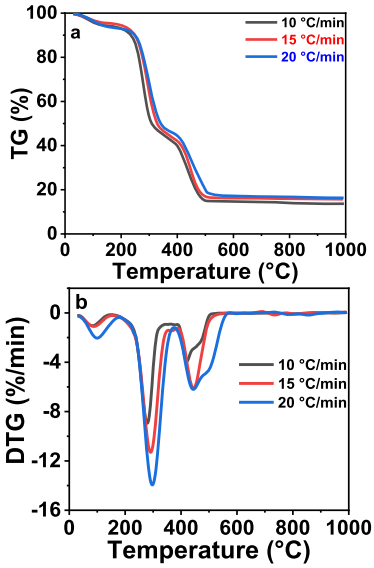

Figure 1. TG (a) and DTG (b) curves of CSB at different heating rates.

presents the TG and derivative thermogravimetric (DTG) curves of CSB under different heating rates. The TG curves revealed that changes in weight loss with increasing temperature. In addition, DTG was derived from TG, which shows the derivative weight loss curves. During combustion, the decomposition of hemicellulose and cellulose firstly generates volatile matter and separates. Then, as the ignition temperature is reached, the volatile matter will burn, followed by the combustion of coke produced by the lignin.[31,32]

Figure 1a,b shows that the combustion process of CSB consists of three stages of thermal degradation. The weak peak in the DTG curve indicates that the mass loss in the first stage corresponds to the removal of moisture content, namely, the dehydration stage. Sometimes, it is also accompanied by a loss of the very small amounts of volatile matters. For the heating rate, 10 and 15 °C/min, they were started at 30 °C and ended at 150 and 155 °C, leading to a mass loss of 5.7 and 4.5%, respectively. Different from the above, the heating rate of 20 °C/min started at 30 °C and ended at 175 °C, leading to a mass loss of 6.7%. It can be seen from Figure 1b that the maximum mass loss in the first stage for the heating rate of 10 and 15 °C/min was 1.03 and 1.10%/min, which occurred at

https://doi.org/10.1021/acsomega.1c01249
ACS Omega 2021, 6, 15827−15833

approximately 85 °C, respectively. In contrast, the maximum weight loss is 2.04%/min for a heating rate of 20 °C/min, which occurred at 100 °C. Next are considered as the main reaction stage during combustion. The second stage corresponds to the combustion of volatile matter generated by the decomposition of hemicellulose, cellulose. The thermal degradation occurred at various temperature zones ranging from 150 to 345 °C, 155 to 355 °C, and 175 to 375 °C for the heating rates of 10, 15, and 20 °C/min, contributing to 48.79, 49.37, and 47.00% of the mass loss, respectively. The DTG curve reveals that the maximum mass loss in stage 2 was 8.96, 11.31, and 13.95%/min for the heating rate of 10, 15, and 20 °C/min, which occurred at a temperature of 278, 290, and 298 °C, respectively. Those conclusions are also similar to the study of Xu et al., Braga et al., and Ahmad et al.[26,33,34] The third stage ranging from 345 to 510 °C, 355 to 545 °C, and 375 to 570 °C under heating rate 10, 15, and 20 °C/min, resulting in the mass loss of 33.88, 33.07, and 29.68%/min, respectively. It was due to the combustion of the char remaining after devolatilization of the samples.

The combustion characteristic parameters, including ignition temperature, burnout temperature, and so forth, obtained from the graph are summarized in Table 2. As presented in Table 2,

Table 2. Combustion Characteristic Parameters

heating rate (°C/min)	10	15	20
ignition temperature (°C)	241	248	248
burnout temperature (°C)	343	368	393
maximum burning rate (%/min)	8.96	11.31	13.95
average burning rate (%/min)	0.042	0.056	0.062
combustion characteristic index (10^{-8})	1.9	2.8	3.6

the data showed clearly that nearly all the parameters increase with the rise of heating rate. While compared to 10 °C/min, the S_n value of CSB increased by 1.5 and 1.9 times at a heating rate of 15 and 20 °C/min, respectively, indicating that the heating rate contributes to the improvement of the combustion performance of CSB.

2.3. Effect of Heating Rates. It is reported that the heating rate has a significant effect on the combustion process. It can affect the maximum decomposition rate, DTG peak temperature, and final residual mass after the combustion.[35−37] Depending on the heating rate, the burnouts are achieved quicker at a lower temperature or later at a higher temperature.[11]

Figure 1a,b vividly describes the effect of heating rate on the biomass briquette combustion at various heating rates of 10, 15, and 20 °C/min. Table 3 reveals that as the heating rate rises from 10 to 20 °C/min, the maximum decomposition rate increases from 8.95 to 13.95%/min, and the DTG peak temperature rises from 278 to 298 °C, which is similar to the study of Jayaraman et al.,[38] in which the peak temperature of DTG curves was shifted to a higher value with an increase in heating rate. This is mainly due to the increase in heating rate; there is a certain difference between the internal and external temperatures of the experimental sample. It takes a long time to transfer the external heat to the internal. Thus, the hysteresis effect occurred.

Table 3. Maximum Decomposition Rate, DTG Peak Temperature, and Final Residual Mass at Different Heating Rates

heating rate (°C/min)	maximum decomposition rate (%/min)	peak temperature (°C)	residual mass (%)
10	8.95	278	14.91
15	11.31	290	16.30
20	13.95	298	17.32

It can be seen from Table 3 that the residual mass increases from 14.91 to 17.32% with the rise of heating rate from 10 to 20 °C/min. It was due to the fact that the lower heating rate helps transfer heat into the interior of CSB, resulting in better combustion. This is also the reason why the termination temperature of every stage observed in Part 2.2 increases with the rise of the heating rate.

2.4. Kinetic Analysis. The combustion process can be displayed through the activation energy ranges with the conversion degree. Here, the activation energy is the energy required to transform molecules from normality to an active state in which the reaction can easily occur. Briefly, it is the minimum energy required for a reaction, whose reaction process takes place easily with lower activation energy than that of higher activation energy.

As mentioned above, the kinetic parameters were determined using isoconversional methods KAS and OFW based on the thermogravimetric analysis data obtained under different heating rates. Figure 2 shows the linear fitting plots of

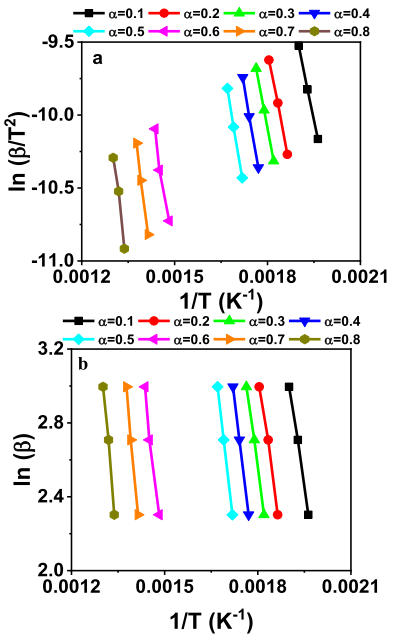

Figure 2. Linear fitting at various α by (a) KAS and (b) OFW methods.

CSB by KAS and OFW methods. Figure 2a shows the linear fitting plot of $\ln\left(\frac{\beta}{T^2}\right)$ versus $\frac{1}{T}$ at the various conversion rates. Similarly, Figure 2b gives the linear fitting plot of $\ln(\beta)$ versus $\frac{1}{T}$ at various conversion degrees. The conversion rate was chosen ranging from 0.1 to 0.8 with a step size of 0.1. For the low coefficient of determination (R^2), a conversion rate beyond 0.8 was not considered. The calculated activation energies from the slopes and intercepts of the plots are listed in Table 4.

https://doi.org/10.1021/acsomega.1c01249
ACS Omega 2021, 6, 15827−15833

Table 4. Calculated Activation Energies of CSB

conversion rate (α)	KAS E (kJ/mol)	KAS R^2	OFW E (kJ/mol)	OFW R^2	difference (%)
0.1	85.67	0.99	88.54	0.99	3.35
0.2	90.34	0.99	92.12	0.99	1.97
0.3	93.14	0.99	96.93	0.99	4.07
0.4	102.15	0.99	109.07	0.99	6.77
0.5	106.58	0.99	114.84	0.99	7.75
0.6	110.95	0.97	116.88	0.98	5.34
0.7	138.95	0.99	145.86	0.99	4.97
0.8	143.01	0.97	151.15	0.99	5.69
average	108.85		114.42		5.12

From Table 4, it can be seen that all the coefficients of determination are larger than 0.97, which indicated the accuracy of the isoconversional methods. In other words, the results of activation energies calculated by the KAS and OFW methods were reliable. The mean activation energy was calculated as 108.85 kJ/mol of the KAS method and 114.42 kJ/mol of the OFW method, respectively. Comparing the two methods, it shows that the difference in average activation energy between KAS and OFW methods was 5.12%. This is consistent with other literature, such as hazelnut husk (7.32%).[4]

The relationship between the activation energy versus the conversion rate is depicted in Figure 3. It can be observed that

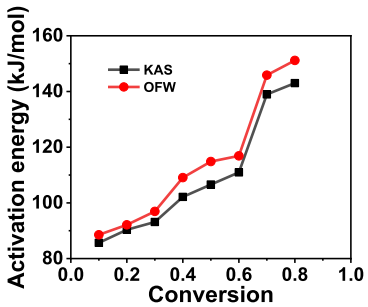

Figure 3. Activation energy vs conversion rate.

changes in the activation energy deeply depended on the conversion rate, reflecting that the combustion process was complex.[35] As shown in Figure 3, the activation energy increased with the increase of conversion rate, regardless of the KAS or OFW method. With the increase of the conversion rate from 0.1 to 0.8, the activation energy ranged from 85.67 to 143.01 kJ/mol for the KAS method and 88.54 to 151.15 kJ/mol for the OFW method. The change in activation energy with the degree of conversion is essentially the result of thermal degradation of different components of biomass with increasing temperature. The weaker bonds (lower molecular weight compounds) decayed at moderate energy and lesser temperature, while degradation of stronger bonds (higher molecular weight products) needed more energy at greater temperature.

Generally, activation energy is regarded as the minimum energy requirement during the reaction.[4] Lower activation energy means faster reaction and vice versa. The kinetic parameter variation with conversion rate is referred to biomass heterogeneity. That is to say, each component has its particular characteristics, thus causing the different phenomenon of various biomass briquette.[39] The interplay of multiple reaction mechanisms leads to a change in activation energy with the degree of conversion. For CSB, the increasing higher activation energy might be caused by the decomposition of chars. A study of Oyedun et al. showed that the chars in biomass had a higher activation energy.[40]

3. CONCLUSIONS

In this study, the combustion and thermal characteristics of corn straw briquette under three heating rates using TGA were investigated. The higher heating value and lower sulfur and nitrogen indicated that the corn straw briquette was a potential fuel. The less residual after combustion in lower heating rate was due to the better heat transfer to the interior of the corn straw briquette. With increasing heating temperature, the maximum thermal decomposition temperature shifted to a higher temperature. In addition, it also leads to the improvement of combustion performance. The combustion kinetics reveals a similar mean activation energy, 108.85 kJ/mol, calculated from the KAS method, and 114.42 kJ/mol calculated from the OFW method. High relation between conversion degree and activation energy indicated the complex combustion process. Based on these above conclusions, it provides the theoretical foundation for future application of corn straw briquette as a fuel resource of energy.

4. MATERIALS AND METHODS

4.1. Materials. Agriculture biomass (corn straw) was locally collected in Zibo city (36.81 °N, 118.05 °E), Shandong province, China. The fresh feedstocks were air-dried for 7 days and then crushed and sieved to less than 0.5 mm particle size. Subsequently, they were dried at 105 °C for 12 h to a constant weight in a drying cabinet and later stored in the ventilated surroundings for briquette preparation.

The briquettes were obtained using a ram compression molding machine described in our patent.[23] Briefly, the raw material was introduced to the forming mold by the screw conveyor and then stroked by a reciprocating plunger to form a briquette. Figure 4 shows a photograph of briquette. For convenience, corn straw briquette was abbreviated as CSB.

4.2. Characteristic Analysis. Proximate analysis for CSB was carried out according to the Chinese standard GB/T 28731-2012. Ultimate analysis of carbon (C), hydrogen (H), nitrogen (N), and sulfur (S) was determined using the

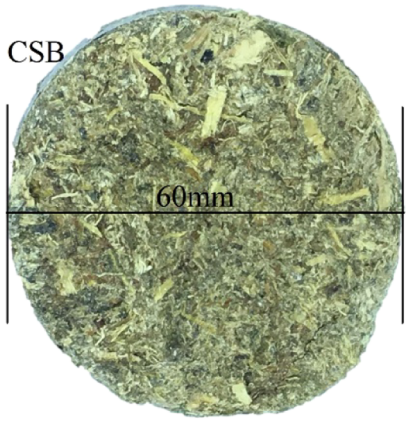

Figure 4. Morphology of CSB.

https://doi.org/10.1021/acsomega.1c01249
ACS Omega 2021, 6, 15827−15833

elemental analyzer (Vario EL Cube). The weight percent of oxygen (O) was determined by difference according to eq 1.

$$O\ \% = 1 - (C + H + N + S)\% \quad (1)$$

All the proximate and ultimate analysis results are presented in Table 1.

4.3. Thermogravimetry Analysis. The combustion was conducted using a thermogravimetric analyzer (Netzsch, STA 449 F5). Approximately 10 mg sample was placed in an aluminum crucible and heated from room temperature (about 26 °C) to 1000 °C with three heating rates (10, 15, and 20 °C/min). The airflow rate was maintained at 20 mL/min.

4.3.1. Combustion Characteristic Parameters. The combustion characteristic parameters mainly refer to ignition temperature (T_i), burnout temperature (T_f), and combustion characteristic index (S_N). They were defined by analyzing the thermogravimetric (TG) curve and DTG curve.

The ignition temperature (T_i) and burnout temperature (T_f) were determined by the TG−DTG joint definition method as presented in Figure 5.[41,42] First, a vertical green line was

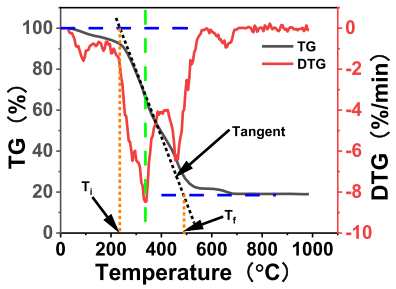

Figure 5. Determination of ignition temperature (T_i) and burnout temperature (T_f).

plotted through the peak point of the DTG curve to meet the TG curve. Then, a tangent was made to the intersection. Finally, the temperature corresponding to the intersection of the tangent and upper horizontal blue line (it was defined as the TG curve begins to lose weight) was recorded as the ignition temperature.

Similarly, the temperature corresponding to the intersection of the tangent and the lower horizontal blue line (it was defined as the end of weight loss of the TG curve) was recorded as the burnout temperature.

As an important indicator of combustion performance, the combustion characteristic index (S_N) was calculated according to eq 2.[43,44]

$$S_N = \frac{(d\alpha/dt)_{max}(d\alpha/dt)_{mean}}{T_i^2 T_f} \quad (2)$$

where $(d\alpha/dt)_{max}$ (%/min) is the maximum burning rate, $(d\alpha/dt)_{mean}$ (%/min) is the average burning rate, and T_i and T_f are the ignition and burnout temperatures, respectively.

Meanwhile, the average burning rate was determined as eq 3.

$$(d\alpha/dt)_{mean} = \beta \times \frac{\alpha_i - \alpha_f}{T_f - T_i} \quad (3)$$

where β is the heating rate, α_i is the percentage of the remaining samples corresponding to ignition temperature, and α_f is the percentage of the remaining samples corresponding to burnout temperature.

4.3.2. Study of Kinetic Modeling. During thermal decomposition, the reaction process can be described as follows

$$\text{Biomass} \rightarrow \text{volatiles} + \text{gas} + \text{biochar}$$

The precipitation rate of volatiles, also named the reaction rate, can be expressed as follows

$$\frac{d\alpha}{dt} = k(T)f(\alpha) \quad (4)$$

where α is the rate of conversion during thermal decomposition, $\frac{d\alpha}{dt}$ is the reaction rate, t is time, T is the absolute temperature, $k(T)$ is the temperature-dependent rate constant, and $f(\alpha)$ is the reaction model.

Moreover, α can be written as follows

$$\alpha = \frac{m_i - m_t}{m_i - m_f} \quad (5)$$

where m_i is the initial mass of the experimental sample before combustion, m_t is the mass of experimental sample at any time t during combustion, and m_f is the final mass of the experimental sample at the end of the combustion.

Here, introducing the Arrhenius laws

$$k(T) = A\exp\left(\frac{-E}{RT}\right) \quad (6)$$

where A is the pre-exponential factor, E (J/mol) is the activation energy of the combustion, R (J/k·mol) is the gas constant, and T (K) is the absolute temperature.

Thus, combining eqs 4 and 6, it then can be rearranged as follows

$$\frac{d\alpha}{dt} = A\exp\left(\frac{-E}{RT}\right)f(\alpha) \quad (7)$$

In addition, the temperature increases with a constant heating value. Then, take $\beta = \frac{dT}{dt} = \frac{dT}{d\alpha} \times \frac{d\alpha}{dt}$ into eq 7. Hence, eq 7 can be rearranged as follows

$$\frac{d\alpha}{dT} = \frac{A}{\beta}\exp\left(\frac{-E}{RT}\right)f(\alpha) \quad (8)$$

Following is the integration function of eq 8.

$$\int_0^\alpha \frac{1}{f(\alpha)}d\alpha = \int_0^T \frac{A}{\beta}\exp\left(\frac{-E}{RT}\right)dT = \frac{AE}{\beta R}$$
$$\int_x^\infty u^{-2}e^{-u}du = \frac{AE}{\beta R}p(x)$$

4.4. KAS Method. The KAS method is presented as follows[45,46]

$$\ln\left(\frac{\beta}{T^2}\right) = \ln\left(\frac{AE}{Rg(x)}\right) - \frac{E}{RT}$$

While plotting the $\ln\left(\frac{\beta}{T^2}\right)$ vs $\frac{1}{T}$, a straight line can be drawn and the slope of the fitted curve is equal to $-\frac{E}{R}$, then E can be calculated.

4.5. OFW Method. The OFW method is presented as follows[47,48]

https://doi.org/10.1021/acsomega.1c01249
ACS Omega 2021, 6, 15827−15833

$$\ln \beta = \ln\left(\frac{AE}{Rg(x)}\right) - 5.331 - 1.052\left(\frac{E}{RT}\right)$$

where the plot of $\ln\beta$ against $\frac{1}{T}$ can be drawn, and the slope of the fitted curve is equal to $-1.052\frac{E}{R}$, then E can be calculated.

AUTHOR INFORMATION

Corresponding Author

Hongzhen Cai − *School of Agricultural Engineering and Food Science, Shandong University of Technology, Zibo, Shandong 255049, China; Shandong Research Center of Engineering and Technology for Clean Energy, Zibo, Shandong 255049, China*; Email: chzh666666@126.com

Authors

Jianbiao Liu − *School of Agricultural Engineering and Food Science, Shandong University of Technology, Zibo, Shandong 255049, China; Shandong Research Center of Engineering and Technology for Clean Energy, Zibo, Shandong 255049, China*; orcid.org/0000-0001-7989-5799

Xuya Jiang − *School of Agricultural Engineering and Food Science, Shandong University of Technology, Zibo, Shandong 255049, China; Shandong Research Center of Engineering and Technology for Clean Energy, Zibo, Shandong 255049, China*

Feng Gao − *Zibo Energy Research Institute, Zibo, Shandong 255049, China*

Complete contact information is available at: https://pubs.acs.org/10.1021/acsomega.1c01249

Notes

The authors declare no competing financial interest.

ACKNOWLEDGMENTS

The authors thank the financial support by the Foundation of Rikaze Science and Technology Plan Project (RKZ2020KJ03).

REFERENCES

(1) Liu, J.; Cheng, W.; Jiang, X.; Khan, M. U.; Zhang, Q.; Cai, H. Effect of extractives on the physicochemical properties of biomass pellets: Comparison of pellets from extracted and non-extracted sycamore leaves. *BioResources* **2020**, *15*, 544−556.

(2) Zhou, C.; Liu, G.; Wang, X.; Qi, C. Co-combustion of bituminous coal and biomass fuel blends: Thermochemical characterization, potential utilization and environmental advantage. *Bioresour. Technol.* **2016**, *218*, 418−427.

(3) Wang, Q.; Wang, G.; Zhang, J.; Lee, J.-Y.; Wang, H.; Wang, C. Combustion behaviors and kinetics analysis of coal, biomass and plastic. *Thermochim. Acta* **2018**, *669*, 140−148.

(4) Ceylan, S.; Topçu, Y. Pyrolysis kinetics of hazelnut husk using thermogravimetric analysis. *Bioresour. Technol.* **2014**, *156*, 182−188.

(5) Sudha, P.; Ravindranath, N. H. Land availability and biomass production potential in India. *Biomass Bioenergy* **1999**, *16*, 207−221.

(6) Pradhan, P.; Mahajani, S. M.; Arora, A. Production and utilization of fuel pellets from biomass: A review. *Fuel Process. Technol.* **2018**, *181*, 215−232.

(7) Saidur, R.; Abdelaziz, E. A.; Demirbas, A.; Hossain, M. S.; Mekhilef, S. A review on biomass as a fuel for boilers. *Renew. Sust. Energ. Rev.* **2011**, *15*, 2262−2289.

(8) Whittaker, C.; Shield, I. Factors affecting wood, energy grass and straw pellet durability - A review. *Renew. Sust. Energ. Rev.* **2017**, *71*, 1−11.

(9) Kaliyan, N.; Vance Morey, R. Factors affecting strength and durability of densified biomass products. *Biomass Bioenergy* **2009**, *33*, 337−359.

(10) Muazu, R. I.; Stegemann, J. A. Effects of operating variables on durability of fuel briquettes from rice husks and corn cobs. *Fuel Process. Technol.* **2015**, *133*, 137−145.

(11) Islam, M. A.; Auta, M.; Kabir, G.; Hameed, B. H. A thermogravimetric analysis of the combustion kinetics of karanja (Pongamia pinnata) fruit hulls char. *Bioresour. Technol.* **2016**, *200*, 335−341.

(12) Haykırı-Açma, H. Combustion characteristics of different biomass materials. *Energy Convers. Manage.* **2003**, *44*, 155−162.

(13) Mian, I.; Li, X.; Dacres, O. D.; Wang, J.; Wei, B.; Jian, Y.; Zhong, M.; Liu, J.; Ma, F.; Rahman, N. Combustion kinetics and mechanism of biomass pellet. *Energy* **2020**, *205*, 117909.

(14) Bach, Q.-V.; Chen, W.-H. A comprehensive study on pyrolysis kinetics of microalgal biomass. *Energy Convers. Manage.* **2017**, *131*, 109−116.

(15) Ma, P.; Yang, J.; Xing, X.; Weihrich, S.; Fan, F.; Zhang, X. Isoconversional kinetics and characteristics of combustion on hydrothermally treated biomass. *Renewable Energy* **2017**, *114*, 1069−1076.

(16) Mishra, R. K.; Mohanty, K. Kinetic analysis and pyrolysis behaviour of waste biomass towards its bioenergy Potential. *Bioresour. Technol.* **2020**, *311*, 123480.

(17) Maia, A. A. D.; de Morais, L. C. Kinetic parameters of red pepper waste as biomass to solid biofuel. *Bioresour. Technol.* **2016**, *204*, 157−163.

(18) Yuan, R.; Yu, S.; Shen, Y. Pyrolysis and combustion kinetics of lignocellulosic biomass pellets with calcium-rich wastes from agro-forestry residues. *Waste Manag.* **2019**, *87*, 86−96.

(19) Jiang, L.; Yuan, X.; Li, H.; Xiao, Z.; Liang, J.; Wang, H.; Wu, Z.; Chen, X.; Zeng, G. Pyrolysis and combustion kinetics of sludge-camphor pellet thermal decomposition using thermogravimetric analysis. *Energy Convers. Manage.* **2015**, *106*, 282−289.

(20) Braga, R. M.; Costa, T. R.; Freitas, J. C. O.; Barros, J. M. F.; Melo, D. M. A.; Melo, M. A. F. Pyrolysis kinetics of elephant grass pretreated biomasses. *J. Therm. Anal. Calorim.* **2014**, *117*, 1341−1348.

(21) Huang, X.; Cao, J.-P.; Zhao, X.-Y.; Wang, J.-X.; Fan, X.; Zhao, Y.-P.; Wei, X.-Y. Pyrolysis kinetics of soybean straw using thermogravimetric analysis. *Fuel* **2016**, *169*, 93−98.

(22) Tahir, M. H.; Zhao, Z.; Ren, J.; Rasool, T.; Naqvi, S. R. Thermo-kinetics and gaseous product analysis of banana peel pyrolysis for its bioenergy potential. *Biomass Bioenergy* **2019**, *122*, 193−201.

(23) Cheng, W. D.; Liu, J. B.; Cai, H. Z.; Jiang, X. Y.; Yi, W. M. Flat-die plunger type biomass solidifying forming machine. CN 201910715788.7, 2020.

(24) Mckendry, P. Energy production from biomass (Part 1): Overview of biomass. *Bioresour. Technol.* **2002**, *83*, 37−46.

(25) Ahmad, M. S.; Mehmood, M. A.; Al Ayed, O. S.; Ye, G.; Luo, H.; Ibrahim, M.; Rashid, U.; Arbi Nehdi, I.; Qadir, G. Kinetic analyses and pyrolytic behavior of Para grass (Urochloa mutica) for its bioenergy potential. *Bioresour. Technol.* **2017**, *224*, 708−713.

(26) Ahmad, M. S.; Mehmood, M. A.; Ye, G.; Al-Ayed, O. S.; Ibrahim, M.; Rashid, U.; Luo, H.; Qadir, G.; Nehdi, I. A. Thermogravimetric analyses revealed the bioenergy potential of Eulaliopsis binata. *J. Therm. Anal. Calorim.* **2017**, *130*, 1237−1247.

(27) Boubacar Laougé, Z.; Merdun, H. Pyrolysis and combustion kinetics of Sida cordifolia L. using thermogravimetric analysis. *Bioresour. Technol.* **2020**, *299*, 122602.

(28) Toptas, A.; Yildirim, Y.; Duman, G.; Yanik, J. Combustion behavior of different kinds of torrefied biomass and their blends with lignite. *Bioresour. Technol.* **2015**, *177*, 328−336.

(29) Jiang, X.; Cheng, W.; Liu, J.; Xu, H.; Zhang, D.; Zheng, Y.; Cai, H. Effect of moisture content during preparation on the physicochemical properties of pellets made from different biomass materials. *BioResources* **2020**, *15*, 557−573.

(30) Zhou, Z.; Hu, X.; You, Z.; Wang, Z.; Zhou, J.; Cen, K. Oxy-fuel combustion characteristics and kinetic parameters of lignite coal from thermo-gravimetric data. *Thermochim. Acta* **2013**, *553*, 54−59.
(31) Worasuwannarak, N.; Sonobe, T.; Tanthapanichakoon, W. Pyrolysis behaviors of rice straw, rice husk, and corncob by TG-MS technique. *J. Anal. Appl. Pyrolysis* **2007**, *78*, 265−271.
(32) Yan, R.; Yang, H.; Chin, T.; Liang, D. T.; Chen, H.; Zheng, C. Influence of temperature on the distribution of gaseous products from pyrolyzing palm oil wastes. *Combust. Flame* **2005**, *142*, 24−32.
(33) Xu, Y.; Chen, B. Investigation of thermodynamic parameters in the pyrolysis conversion of biomass and manure to biochars using thermogravimetric analysis. *Bioresour. Technol.* **2013**, *146*, 485−493.
(34) Braga, R. M.; Melo, D. M. A.; Aquino, F. M.; Freitas, J. C. O.; Melo, M. A. F.; Barros, J. M. F.; Fontes, M. S. B. Characterization and comparative study of pyrolysis kinetics of the rice husk and the elephant grass. *J. Therm. Anal. Calorim.* **2014**, *115*, 1915−1920.
(35) Bhattacharjee, N.; Biswas, A. B. Physicochemical analysis and kinetic study of orange bagasse at higher heating rates. *Fuel* **2020**, *271*, 117642.
(36) Ranjith Kumar, R.; Ramesh, D.; Mutanda, T.; Rawat, I.; Bux, F. Thermal Behavior and Pyrolytic Characteristics of FreshwaterScene-desmussp. Biomass. *Energy Sources, Part A* **2015**, *37*, 1383−1391.
(37) Thakur, L. S.; Varma, A. K.; Mondal, P. Analysis of thermal behavior and pyrolytic characteristics of vetiver grass after phytoremediation through thermogravimetric analysis. *J. Therm. Anal. Calorim.* **2018**, *131*, 3053−3064.
(38) Jayaraman, K.; Kök, M. V.; Gökalp, I. Combustion mechanism and model free kinetics of different origin coal samples: Thermal analysis approach. *Energy* **2020**, *204*, 117905.
(39) Rahib, Y.; Sarh, B.; Bostyn, S.; Bonnamy, S.; Boushaki, T.; Chaoufi, J. Non-isothermal kinetic analysis of the combustion of argan shell biomass. *Mater. Today: Proc.* **2020**, *24*, 11−16.
(40) Oyedun, A. O.; Tee, C. Z.; Hanson, S.; Hui, C. W. Thermogravimetric analysis of the pyrolysis characteristics and kinetics of plastics and biomass blends. *Fuel Process. Technol.* **2014**, *128*, 471−481.
(41) Yuanyuan, Z.; Yanxia, G.; Fangqin, C.; Kezhou, Y.; Yan, C. Investigation of combustion characteristics and kinetics of coal gangue with different feedstock properties by thermogravimetric analysis. *Thermochim. Acta* **2015**, *614*, 137−148.
(42) Ma, B.-G.; Li, X.-G.; Xu, L.; Wang, K.; Wang, X.-G. Investigation on catalyzed combustion of high ash coal by thermogravimetric analysis. *Thermochim. Acta* **2006**, *445*, 19−22.
(43) Essenhigh, R. H.; Misra, M. K.; Shaw, D. W. Ignition of coal particles: a review. *Combust. Flame* **1989**, *77*, 3−30.
(44) Zhao, D.; Zhang, J.; Wang, G.; Conejo, A. N.; Xu, R.; Wang, H.; Zhong, J. Structure characteristics and combustibility of carbonaceous materials from blast furnace flue dust. *Appl. Therm. Eng.* **2016**, *108*, 1168−1177.
(45) Akahira, T.; Sunuse, T. T. *Joint Convention of Four Electrical Institutes, Research Report*; Chiba Institute of Technology, 1971; Vol. *16*; pp 22−31.
(46) Kissinger, H. E. Reaction Kinetics in Differential Thermal Analysis. *Anal. Chem.* **1957**, *29*, 1702−1706.
(47) Ozawa, T. A New Method of Analyzing Thermogravimetric Data. *Bull. Chem. Soc. Jpn.* **1965**, *38*, 1881−1886.
(48) Flynn, J. H.; Wall, L. A. A quick, direct method for the determination of activation energy from thermogravimetric data. *J. Polym. Sci., Part B: Polym. Lett.* **1966**, *4*, 323−328.

https://doi.org/10.1021/acsomega.1c01249
ACS Omega 2021, 6, 15827−15833